

Quantum interference along satellite-ground channels

Giuseppe Vallone,¹ Daniele Dequal,¹ Marco Tomasin,¹ Francesco Vedovato,¹
Matteo Schiavon,¹ Vincenza Luceri,² Giuseppe Bianco,³ and Paolo Villoresi^{1, *}

¹*Dipartimento di Ingegneria dell'Informazione, Università degli Studi di Padova, Padova, Italy*
²*e-GEOS spa, Matera, Italy*

³*Matera Laser Ranging Observatory, Agenzia Spaziale Italiana, Matera, Italy*
(Dated: September 28, 2015)

Observing quantum interference by moving terminals in Space is a great challenge as well as a necessary tool for testing Quantum Mechanics in an unexplored scenario. Here we experimentally demonstrate single photon interference due to a superposition of two temporal modes reflected by a rapidly moving satellite thousand kilometers away from the ground station. The relative speed of the satellite induces a varying modulation in the interference pattern. The measurement of the satellite distance in real time by laser ranging allowed us to precisely predict the instantaneous value of the interference phase. We observed the interference patterns with visibility up to 67% with three different satellites. Our results pave the way for Quantum Communications and tests of Quantum Mechanics and General Relativity.

Quantum interference is playing a crucial role to highlight the essence of Quantum Mechanics since the Einstein-Bohr dialogues at the end of the Twenties [1]. Individual particles can be in more than one place at any given time, the so called quantum superposition. Such superposition can indeed be verified by measuring interference between *alternative possibilities*. Quantum interference can be observed with photons [2, 3], electrons [4], neutrons [5] and even with large molecules with masses exceeding 10000 amu [6]. One of the main challenges in Quantum Physics is establishing if fundamental bounds to interference exist: for instance, can we observe quantum interference at arbitrary large distance and with components in relative motion?

We address this question by exploiting temporal modes of photon to demonstrate the interference along satellite-ground channels. To this purpose, we generated a quantum superposition and observed its interference after a reflection by a rapidly moving satellite at very large distance. The relative speed of the satellite with respect to the ground introduces a modulation in the interference pattern, as explained below. Our results show that interference can be observed with fast moving objects, paving the way for Quantum Communications (QC) and tests of Quantum Mechanics combined with General Relativity.

The interplay of Quantum Theory with Gravitation is indeed one of the big unresolved puzzle in Physics. Novel experimental schemes are needed to reveal the effect of Gravity in quantum experiments. These include the exchange of elementary particles from moving and accelerated reference frames, which would allow to test Bell's inequalities, quantum interference and possible gravity-induced decoherence in this novel scenario [7, 8]. We point out that tiny gravitational effects may be enhanced by increasing the temporal separation of the two interfering modes unlike the case of effects manifested by photon polarization rotation as in the scheme proposed in the optical version [7, 9] of the Colella-Overhauser-Werner

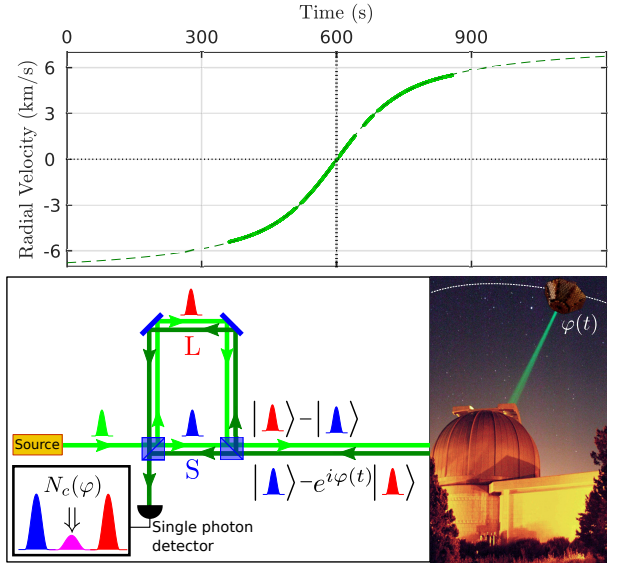


FIG. 1. *Scheme of the experiment and satellite radial velocity.* In the top panel we show the measured radial velocity of the Beacon-C satellite ranging from -6 km/s to $+6$ km/s as a function of time during a single passage. Dashed line represents the fit. In the bottom panel we show the unbalanced MZI used for the generation of quantum superposition and the measurement of quantum interference. Light and dark green lines represents outgoing and ingoing beam respectively. Right photo shows MLRO with the laser ranging beam and the Beacon-C satellite (not to scale). The phase $\varphi(t)$ depends on the satellite radial velocity as described in the text.

(COW) experiment realized with neutrons [10]: gravitational phase shift between a superposition of two photon wavepackets could provide tests of gravitational redshift in the context of a quantum optics experiment.

In our scheme, a superposition $|\Psi_{\text{out}}\rangle$ between two photon wavepackets $|S\rangle$ and $|L\rangle$ is generated at the ground station with an unbalanced Mach-Zehnder interferome-

ter (MZI), sketched in the lower panel of Fig. 1. The delay $\Delta t \simeq 3.4$ ns between the two wavepackets corresponds to a length difference between the two arms of $\ell = c\Delta t \simeq 1$ m (c is the speed of light in vacuum) and it is much longer than the coherence time $\tau_c \approx 83$ ps of each wavepacket (we used the convention of [11] for the definition of τ_c). The superposition of two photon wavepackets separated in time is also known as *time-bin encoding*, and it is used for both fundamental tests ([12–15]) as well as for Quantum Information applications such as quantum key distribution (QKD) along optical fibers ([16, 17]).

Using a telescope, the state $|\Psi_{\text{out}}\rangle$ is directed to a retroreflector placed on a satellite in orbit. The satellite instantaneous radial velocity with respect to ground, $v_r(t)$, is shown in the top panel of Fig 1, in the case of a passage of the Beacon-C satellite. At a given instant t , the satellite motion determines a slipping of the reflector position, during the separation Δt between the two wavepackets, that can be assessed (at the first order) as $\Delta x_r(t) \approx v_r(t)\Delta t$. Therefore, the satellite motion imposes during reflection an additional *kinematic phase* $\varphi(t) \approx \frac{2\pi}{\lambda}(2\Delta x_r(t))$ between the wavepackets $|L\rangle$ and $|S\rangle$, where λ is the pulse wavelength in vacuum. The state reflected by the satellite may be written as $|\Psi_r\rangle = \frac{1}{\sqrt{2}}(|S\rangle - e^{i\varphi(t)}|L\rangle)$. The satellite directs $|\Psi_r\rangle$ back to the ground station, where it is collected and directed to the same MZI used in the uplink. A single MZI for state generation and detection intrinsically ensures the same unbalancement of the arms and avoids active stabilization, necessary otherwise.

The MZI at the receiver is able to reveal the interference between the two returning wavepackets. At the MZI outputs we expect detection times that follow the well known three-peak profile (see Fig. 1): the first peak represents the pulse $|S\rangle$ taking again the short arm, while the third represents the delayed pulse $|L\rangle$ taking again the long arm. In the central peak we expect quantum interference due to the indistinguishability between two *alternative possibilities*: the $|S\rangle$ pulse taking the long arm and the $|L\rangle$ pulse taking the short arm in the path along the MZI toward to detector.

To measure the interference effect we used a single photon detector placed at the available port of the MZI, as shown in Fig. 1. As detailed in Appendix, a special relativistic calculation shows that the probability P_c of detecting the photon in the central peak is given by

$$P_c(t) = \frac{1}{2} [1 - \mathcal{V}(t) \cos \varphi(t)], \quad (1)$$

with

$$\varphi(t) = \frac{2\beta(t)}{1 + \beta(t)} \frac{2\pi c}{\lambda} \Delta t \quad (2)$$

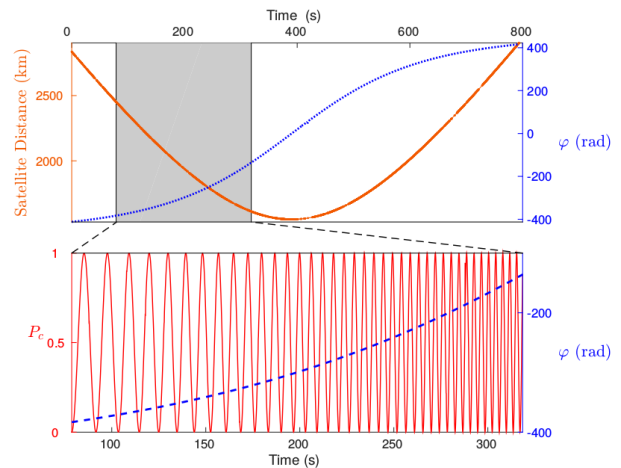


FIG. 2. *Kinematic phase and interference pattern.* Top panel: we show the measured satellite distance and the predicted kinematic phase $\varphi(t)$ estimated by eq. (2) as a function of time. Shaded area represents the temporal window of data acquisition for the Ajisai satellite. Bottom panel: kinematic phase $\varphi(t)$ and theoretical probability $P_c(t)$ in the shaded area. The interference pattern is modulated according to satellite velocity.

and

$$\mathcal{V}(t) = e^{-2\pi\left(\frac{\Delta t}{\tau_c} \frac{\beta(t)}{1+\beta(t)}\right)^2} \simeq 1. \quad (3)$$

In the above relations, $\beta(t)$ is defined as $\beta(t) = \frac{v_r(t)}{c}$. We note that the first order approximation of eq. (2) gives the phase $\varphi(t) \approx \frac{4\pi}{\lambda} v_r(t)\Delta t$ above described. The theoretical visibility $\mathcal{V}(t)$ is approximately 1 since the β factor is upper bounded by $3 \cdot 10^{-5}$ in all the experimental studied cases, while the ratio $\frac{\Delta t}{\tau_c}$ is of the order of 10^2 .

We realized our experiment at the Matera Laser Ranging Observatory (MLRO) of the Italian Space Agency in Matera, Italy, that is equipped with a 1.5 m telescope designed for precise satellite tracking and which acted as ground quantum-hub for the first demonstrations of Space-QC [18, 19].

The pulses used to prepared $|\Psi_{\text{out}}\rangle$ are generated by a mode-locking laser based on Nd:YVO₄ gain medium operating at a repetition rate stabilized at 100 MHz by an atomic clock and at the wavelength of 1064 nm. Each pulse is upconverted with a PPLN crystal to 532 nm. The pulses are sent to the Coudé path of the MLRO telescope, that directs the state $|\Psi_{\text{out}}\rangle$ toward the satellite while actively tracking its orbit. We selected three satellites in low-Earth-orbit (LEO) – Beacon-C, Stella and Ajisai – which are equipped with efficient cube-corner retroreflectors (CCR). Thanks to the CCR properties, the state is automatically redirected toward the ground station, where it is injected into the same MZI used in the uplink.

The value of $\varphi(t)$ originating from the satellite motion

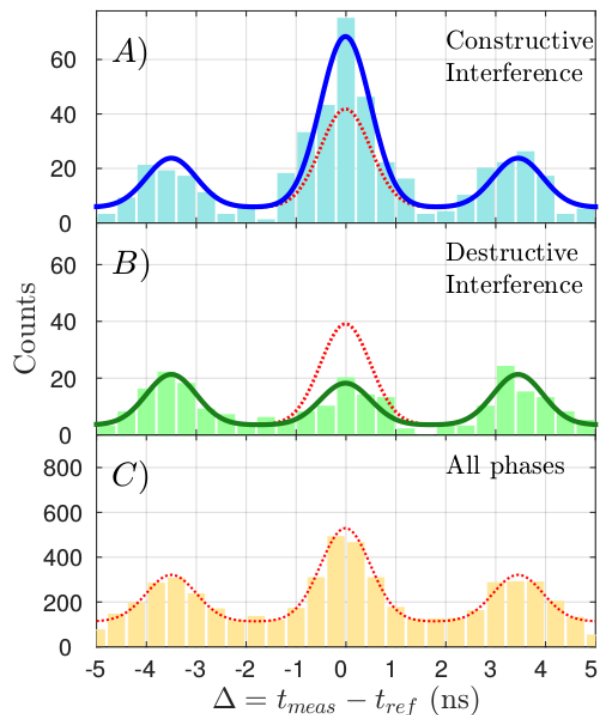


FIG. 3. *Constructive and destructive interference* (Beacon-C satellite, 11.07.2015 h 1.33 CEST). A): histogram of the single photon detections as a function of time $\Delta = t_{meas} - t_{ref}$ realized by selecting only the returns characterized by $\varphi \bmod 2\pi \in [4\pi/5, 6\pi/5]$ that lead to constructive interference. Solid line shows the tri-Gaussian fit. By evaluating the Gaussian integrals we obtained the counts $N_\ell = 112 \pm 11$ for the sum of lateral peaks and $N_c = 196 \pm 14$ for the central one. B): histogram of the single photon detections realized by selecting only the returns characterized by $\varphi \bmod 2\pi \in [-\pi/5, \pi/5]$. Here $N_\ell = 112 \pm 11$ and $N_c = 46 \pm 7$. C): histogram of the single photon detections without any selection on the phase. As expected, interference is completely washed out and we measured $N_c = 1245 \pm 35$ and $N_\ell = 1306 \pm 36$, fully compatible with $P_c = 1/2$. In all panels, dotted red lines represent the expected counts in case of no interference.

can be precisely predicted on the base of the sequence of measurements of the instantaneous distance of the satellite, or *range*, which is realized in parallel. Indeed, by measuring the range every 100 ms, the instantaneous satellite velocity relative to the ground station $v_r(t)$ can be estimated, from which $\varphi(t)$ can be derived by eq. (2). In the top panel of Fig. 2, for a given passage of the Ajisai satellite, we show the measured satellite distance and the estimated $\varphi(t)$ as a function of time from the start to the end of the satellite tracking. Since $v_r(t)$ is continuously changing along the orbit the value of $\varphi(t)$ is varying accordingly. In the bottom panel of Fig. 2 we show the variation of the theoretical output probability $P_c(t)$ along the Ajisai orbit as predicted by eq. (1).

The quantum measurement at the receiver requires a very precise temporal synchronization and a strong rejection

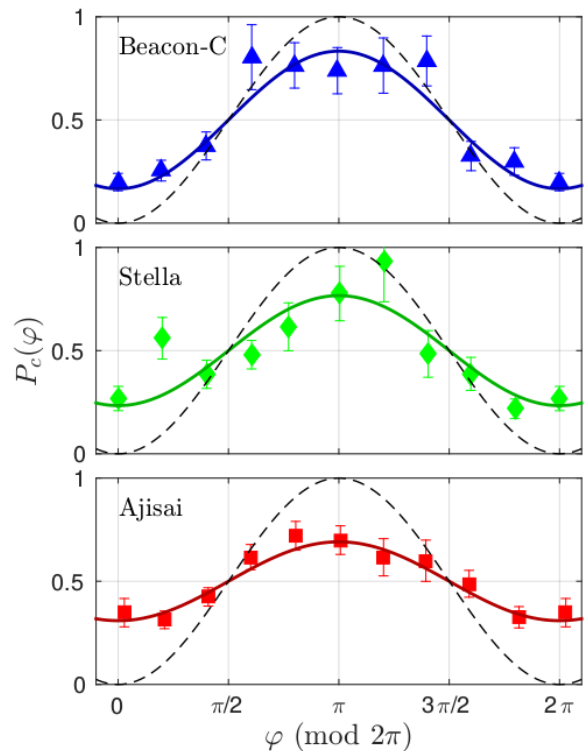


FIG. 4. *Experimental interference pattern*. Experimental probabilities $P_c^{(\text{exp})}$ as a function of the kinematic phase measured for three different satellites. By fitting the data we estimate the visibilities $\mathcal{V}_{\text{exp}} = 67 \pm 11\%$ for Beacon-C, $\mathcal{V}_{\text{exp}} = 53 \pm 13\%$ for Stella and $\mathcal{V}_{\text{exp}} = 38 \pm 4\%$ for Ajisai. Dashed lines correspond to the theoretical value of P_c predicted by (1). The points are obtained by considering ten intervals of the phase defined by $\mathcal{I}_j \equiv [\frac{j-1}{10}\pi, \frac{j+1}{10}\pi]$. For each interval we selected the data corresponding to $\varphi \bmod 2\pi \in \mathcal{I}_j$: from such data we determined the experimental probability of detection in the central peak $P_c^{(\text{exp})}$ and we averaged the corresponding phase φ . We note that at point $\varphi = 0$ and $\varphi = 2\pi$ the same subset of data were selected. The data were collected at the following satellite distance ranges: 1600 ÷ 2500 km (Ajisai, 12.07.2015, h 3.42 CEST), 1100 ÷ 1500 km (Stella, 12.07.2015, h 3.08 CEST) and 1200 ÷ 1500 km (Beacon-C, 11.07.2015, h 1.33 CEST).

tion of the background, necessary to observe the single photon interference. The measurement of the satellite position along the orbit by a laser ranging technique as in Fig. 2 was also essential for the determination of the expected instant of arrival (t_{ref}) of the photons at the MZI output. By using a time-to-digital converter with 81 ps resolution (QuTAU), we acquired the start and stop signals of the laser ranging pulses, together with PMT detections. We denote PMT timestamps as t_{meas} . In this way, we may calculate the histogram of the returns in the temporal window of 10 ns between two consecutive pulses as a function of the temporal difference $\Delta = t_{meas} - t_{ref}$ corresponding to a desired value of $\varphi(t)$.

In Fig. 3 we show the histograms of single photon de-

tections corresponding to constructive and destructive interference in the case of satellite Beacon-C. In particular, for the constructive interference (Fig. 3A) we selected the detections corresponding to $\varphi \bmod 2\pi \in [\frac{4}{5}\pi, \frac{6}{5}\pi]$. For the destructive interference (Fig. 3B) we selected a kinematic phase $\varphi \bmod 2\pi \in [-\frac{1}{5}\pi, \frac{1}{5}\pi]$. The detections in the central peak are respectively higher or lower than the sum of the two lateral peaks in the two cases. We note that the peak width is determined by the detector timing jitter which has standard deviation $\sigma = 0.5$ ns. These two histograms clearly show the interference effect in the central peak. On the contrary, Fig. 3C is obtained by taking all the data without any selection on φ . In this case, the interference is completely washed out. This results shows that, in order to prove the interference effect, it is crucial to correctly predict the kinematic phase φ imposed by the satellite motion. In the caption of Fig. 3 we report the satellite slanted distances, giving two-way channel lengths ranging from 2200 up to 5000 km.

By using the data of Fig. 3, we experimentally evaluate the probability $P_c^{(\text{exp})}$ as the ratio of the detections associated the central peak N_c to two times the sum N_ℓ of the detections associated to the side peaks, namely

$$P_c^{(\text{exp})} = \frac{N_c}{2N_\ell}. \quad (4)$$

The values $P_c^{(\text{exp})} = 0.87 \pm 0.10$ and $P_c^{(\text{exp})} = 0.20 \pm 0.03$ are obtained for constructive and destructive interference respectively. The values deviates with clear statistical evidence from 0.5, which is the expected value in the case of no interference. The mean number of photon μ in the received pulses may be derived by measuring the detection rate and from the optical losses η in the receiving setup. At the primary mirror of the receiving telescope, the average μ during the data acquisition are given by $\mu \approx 7 \cdot 10^{-4}$ for Beacon-C, $\mu \approx 2 \cdot 10^{-3}$ for Ajisai and $\mu \approx 9 \cdot 10^{-4}$ for Stella. From these values we may conclude that interference was probed at the single photon level. Indeed, the probability of having more that one photon per pulse in the receiver MZI is $\eta\mu^2/2$.

Moreover, we evaluated the experimental probabilities $P_c^{(\text{exp})}$ for ten different values of the kinematic phase φ . A more clear evidence of the role of $\varphi(t)$ can be seen in Fig. 4 in which is shown $P_c^{(\text{exp})}$ as a function of φ for the three different satellites. By fitting the data by $P_c^{(\text{exp})} = \frac{1}{2}(1 - \mathcal{V}_{\text{exp}} \cos \varphi)$, we estimated the experimental visibilities $\mathcal{V}_{\text{exp}} = 67 \pm 11\%$ for Beacon-C, $\mathcal{V}_{\text{exp}} = 53 \pm 13\%$ for Stella and $\mathcal{V}_{\text{exp}} = 38 \pm 4\%$ for Ajisai. Such interference clearly demonstrates that the quantum superposition is preserved along these thousand km scale channels with rapidly moving retroreflectors.

In conclusion, quantum interference between two temporal modes of a single photon was observed along a path including a rapidly moving retroreflector on a satellite.

The relative motion of the satellite with respect to the ground induces a varying phase that modulates the interference pattern, which has been effectively experimentally measured. The effect was demonstrated with three satellites, Beacon-C, Stella and Ajisai, having different relative velocities and distances from the ground station.

Up to now, photon polarization was the only degree of freedom exploited in long distance and satellite QC. Indeed, QC along a Space channels of length up to 2000 km have been recently demonstrated by our group using this property [19]. Results here described attest the viability of the use of photon temporal modes for fundamental tests of Quantum Mechanics and global secure communications around the planet and beyond.

We would like to thank Francesco Schiavone, Giuseppe Nicoletti, and the MRLO technical operators for the collaboration and support, Prof. Roberto Regazzoni of INAF-Osservatorio Astronomico di Padova for the useful discussion on the interferometer optics as well as Dr. Davide Bacco and Simone Gaiarin for their contributions to the setup. We also thank Franco Ambrico for the image of MLRO. Our work was supported by the Strategic-Research-Project QUINTET of the Department of Information Engineering, University of Padova, the Strategic-Research-Project QUANTUMFUTURE of the University of Padova.

* paolo.villoresi@dei.unipd.it

- [1] N. Bohr, *Can Quantum-Mechanical Description of Physical Reality Be Considered Complete?*, Phys. Rev. **48**, 696 (1935).
- [2] G. I. Taylor, *Interference fringes with feeble light*, Proceedings of the Cambridge Philosophical Society **15**, 114 (1909).
- [3] P. Grangier, A. Aspect, and J. Vigue, *Quantum Interference Effect for Two Atoms Radiating a Single Photon*, Physical Review Letters **54**, 418 (1985).
- [4] C. Jönsson, *Electron Diffraction at Multiple Slits*, American Journal of Physics **42**, 4 (1974).
- [5] H. Rauch and S. A. Werner, *Neutron Interferometry*, OUP Oxford (2015), ISBN 9780198712510.
- [6] S. Eibenberger, S. Gerlich, M. Arndt, M. Mayor, and J. Tüxen, *Matter-wave interference of particles selected from a molecular library with masses exceeding 10,000 amu*, Physical chemistry chemical physics : PCCP **15**, 14696 (2013).
- [7] D. Rideout, T. Jennewein, G. Amelino-Camelia, T. F. Demarie, B. L. Higgins, A. Kempf, A. Kent, R. Laflamme, X. Ma, R. B. Mann, E. Martín-Martínez, N. C. Menicucci, J. Moffat, C. Simon, R. Sorkin, L. Smolin, and D. R. Terno, *Fundamental quantum optics experiments conceivable with satellites reaching relativistic distances and velocities*, Classical and Quantum Gravity **29**, 224011 (2012).
- [8] G. Ghirardi, R. Grassi, and A. Rimini, *Continuous-spontaneous-reduction model involving gravity*, Physical Review A **42**, 1057 (1990).

- [9] M. Zych, F. Costa, I. Pikovski, and v. Brukner, *Quantum interferometric visibility as a witness of general relativistic proper time*, Nature Communications **2**, 505 (2011).
- [10] R. Colella, A. W. Overhauser, and S. Werner, *Observation of gravitationally induced quantum interference*, Phys. Rev. Lett. **34**, 1472 (1975).
- [11] B. E. A. Saleh and M. C. Teich, *Fundamentals of Photonics*, Wiley (1991).
- [12] J. D. Franson, *Bell inequality for position and time*, Phys. Rev. Lett. **62**, 2205 (1989).
- [13] W. Tittel, J. Brendel, H. Zbinden, and N. Gisin, *Violation of Bell Inequalities by Photons More Than 10 km Apart*, Physical Review Letters **81**, 3563 (1998).
- [14] G. Lima, G. Vallone, A. Chiuri, A. Cabello, and P. Mataloni, *Experimental Bell-inequality violation without the postselection loophole*, Phys. Rev. A **81**, 2 (2010).
- [15] G. Carvacho, J. Cariñe, G. Saavedra, A. Cuevas, J. Fuenzalida, F. Toledo, M. Figueroa, A. Cabello, J.-A. k. Larsson, P. Mataloni, G. Lima, and G. B. Xavier, *Postselection-Loophole-Free Bell Test Over an Installed Optical Fiber Network*, Physical Review Letters **115**, 030503 (2015).
- [16] J. Brendel, N. Gisin, W. Tittel, and H. Zbinden, *Pulsed Energy-Time Entangled Twin-Photon Source for Quantum Communication*, Phys. Rev. Lett. **82**, 2594 (1999).
- [17] N. Gisin, G. Ribordy, W. Tittel, and H. Zbinden, *Quantum cryptography*, Reviews of Modern Physics **74**, 145 (2002).
- [18] P. Villoresi, T. Jennewein, F. Tamburini, M. Aspelmeyer, C. Bonato, R. Ursin, C. Pernechele, V. Luceri, G. Bianco, A. Zeilinger, and C. Barbieri, *Experimental verification of the feasibility of a quantum channel between space and Earth*, New Journal of Physics **10**, 033038 (2008).
- [19] G. Vallone, D. Bacco, D. Dequal, S. Gaiarin, V. Luceri, G. Bianco, and P. Villoresi, *Experimental Satellite Quantum Communications*, Physical Review Letters **115**, 040502 (2015).

Appendix: Interference by mirror moving at constant velocity

Let's consider a single pulse of light whose peak passes at $x = 0$ for $t = 0$. Its wavefunction is given by

$$\psi_0(\tau_-) = \sqrt[4]{\frac{2}{\tau_c^2}} e^{-\pi \frac{\tau_-^2}{\tau_c^2}} e^{i\omega_0 \tau_-} \quad (5)$$

where we have defined the quantities

$$\tau_{\pm} = \frac{x}{c} \pm t \quad (6)$$

and $\omega_0 = \frac{2\pi c}{\lambda}$ is the angular frequency. The parameter τ_c represents the coherence time of the pulse, where we have used the convention of [11], namely

$$\tau_c = \int |g(\tau)|^2 d\tau, \quad (7)$$

and

$$g(\tau) = \langle \psi^*(t) \psi(t + \tau) \rangle = \int_{-\infty}^{+\infty} \psi_0^*(t) \psi_0(t + \tau) e^{i\omega_0 \tau} dt = e^{-\frac{\pi \tau^2}{2\tau_c^2}} e^{i\omega_0 \tau}. \quad (8)$$

If the pulse passes through the unbalanced Mach-Zehnder interferometer shown in Fig. 1 of the main text we obtain

$$\psi_1(\tau_-) = \frac{1}{\sqrt{2}} [\psi_0(\tau_-) - \psi_0(\tau_- - \Delta t)] = \frac{1}{\sqrt{2}\tau_c^2} \left[e^{-\pi \frac{\tau_-^2}{\tau_c^2}} - e^{-\pi \frac{(\tau_- - \Delta t)^2}{\tau_c^2}} \right]$$

where Δt is the unbalancement.

Let's consider a mirror moving at constant velocity with respect to the interferometer that at time $t = 0$ is located at $x = x_M$. We may change reference frame by setting the origin at the location of the mirror. The corresponding

Lorentz transformation are given by

$$\begin{cases} x' = \gamma(x - x_M - \beta ct) \\ t' = \gamma(t - \beta \frac{x - x_M}{c}) \end{cases} \quad \begin{cases} x = x_M + \gamma(x' + \beta ct') \\ t = \gamma(t' + \beta \frac{x'}{c}) \end{cases}$$

The wave function in the mirror reference frame can be derived by the transformations of the τ_{\pm} parameter:

$$\tau_{\pm} = \gamma(1 \pm \beta)\tau'_{\pm} + \frac{x_M}{c} = \sqrt{\frac{1 \pm \beta}{1 \mp \beta}}\tau'_{\pm} + \frac{x_M}{c} \quad (9)$$

The reflection on the mirror can be described simply by the transformation $\tau'_- \rightarrow -\tau'_+$. We now use (9), namely $\tau'_+ = \frac{1}{\gamma(1+\beta)}(\tau_+ - \frac{x_M}{c})$ to go back to the interferometer ref. frame. If we define $t_M = \frac{2}{1-\beta}\frac{x_M}{c}$, the total transformation can be summarized by

$$\begin{aligned} \tau_- &\xrightarrow{\text{boost}} \gamma(1 - \beta)\tau'_- + \frac{x_M}{c} \xrightarrow{\text{reflection}} -\gamma(1 - \beta)\tau'_+ + \frac{x_M}{c} \\ &\xrightarrow{\text{boost back}} -f_{\beta}(\tau_+ - t_M) \end{aligned}$$

with

$$f_{\beta} = \gamma^2(1 - \beta)^2 = \frac{1 - \beta}{1 + \beta}$$

Also the normalization should be changed (to preserve normalization), such that the beam coming back from the satellite is written as

$$\begin{aligned} \psi_2(\tau_+) &= \sqrt{f_{\beta}}\psi_1(-f_{\beta}(\tau_+ - t_M)) \\ &= \frac{\gamma(1 - \beta)}{\sqrt{2}}[\psi_0(-f_{\beta}(\tau_+ - t_M)) - \psi_0(-f_{\beta}(\tau_+ - t_M) - \Delta t)] \end{aligned} \quad (10)$$

We now comment the two terms. The first term is

$$\psi_0(-f_{\beta}(\tau_+ - t_M)) = \sqrt{\frac{2}{\tau_c^2}} e^{-\pi \frac{f_{\beta}^2(\tau_+ - t_M)^2}{\tau_c^2}} e^{-if_{\beta}\omega_0(\tau_+ - t_M)}$$

representing a pulse with stretched temporal width (doppler shift): the new width is indeed

$$\delta' = \frac{\delta}{f_{\beta}} = \frac{1 + \beta}{1 - \beta}\delta > \delta$$

The term t_M represents the time that the pulse peak takes to come back to the origin (namely the round trip time). The second term in (10) represents the same pulse delayed by $\Delta t' = \frac{\Delta t}{f_{\beta}}$.

After passing again in the interferometer we get at the detection port of the MZI the following state:

$$\psi_3(\tau_+ + t_M) = \frac{i\gamma(1 - \beta)}{2} [\psi_0(-f_{\beta}\tau_+) + \psi_0(-f_{\beta}(\tau_+ + \Delta t)) - \psi_0(-\Delta t - f_{\beta}\tau_+) - \psi_0(-\Delta t - f_{\beta}(\tau_+ + \Delta t))]$$

We have three pulses at the detector: the probability of getting the photon in the central pulse at $x = 0$ is given by

$$\begin{aligned} P_c(t) &= \frac{\gamma^2(1 - \beta(t))^2}{4} \int dt' |\psi_0(-f_{\beta}(t' + \Delta t)) - \psi_0(-\Delta t - f_{\beta}t')|^2 \\ &= \frac{1}{2} \left\{ 1 - \sqrt{\frac{2}{\tau_c^2}} \int dt' \Re \left[e^{-\pi \frac{(t' + f_{\beta}\Delta t)^2}{\tau_c^2}} e^{-\pi \frac{(t' + \Delta t)^2}{\tau_c^2}} e^{i\omega_0(1 - f_{\beta})\Delta t} \right] \right\} \\ &= \frac{1}{2} [1 - \mathcal{V}(t) \cos \varphi(t)] \end{aligned} \quad (11)$$

with

$$\varphi(t) = \omega_0[1 - f_\beta]\Delta t = \frac{2\beta(t)}{1 + \beta(t)}\omega_0\Delta t \quad (12)$$

and

$$\mathcal{V}(t) = \sqrt{\frac{2}{\tau_c^2}} \int dt' e^{-\pi \frac{(t'+f_\beta\Delta t)^2}{\tau_c^2}} e^{-\pi \frac{(t'+\Delta t)^2}{\tau_c^2}} = \exp\left\{-2\pi \left[\frac{\Delta t}{\tau_c} \frac{\beta(t)}{1 + \beta(t)}\right]^2\right\} \quad (13)$$

* paolo.villoresi@dei.unipd.it

- [1] N. Bohr, *Can Quantum-Mechanical Description of Physical Reality Be Considered Complete?*, Phys. Rev. **48**, 696 (1935).
- [2] G. I. Taylor, *Interference fringes with feeble light*, Proceedings of the Cambridge Philosophical Society **15**, 114 (1909).
- [3] P. Grangier, A. Aspect, and J. Vigue, *Quantum Interference Effect for Two Atoms Radiating a Single Photon*, Physical Review Letters **54**, 418 (1985).
- [4] C. Jönsson, *Electron Diffraction at Multiple Slits*, American Journal of Physics **42**, 4 (1974).
- [5] H. Rauch and S. A. Werner, *Neutron Interferometry*, OUP Oxford (2015), ISBN 9780198712510.
- [6] S. Eibenberger, S. Gerlich, M. Arndt, M. Mayor, and J. Tüxen, *Matter-wave interference of particles selected from a molecular library with masses exceeding 10,000 amu*, Physical chemistry chemical physics : PCCP **15**, 14696 (2013).
- [7] D. Rideout, T. Jennewein, G. Amelino-Camelia, T. F. Demarie, B. L. Higgins, A. Kempf, A. Kent, R. Laflamme, X. Ma, R. B. Mann, E. Martín-Martínez, N. C. Menicucci, J. Moffat, C. Simon, R. Sorkin, L. Smolin, and D. R. Terno, *Fundamental quantum optics experiments conceivable with satellites reaching relativistic distances and velocities*, Classical and Quantum Gravity **29**, 224011 (2012).
- [8] G. Ghirardi, R. Grassi, and A. Rimini, *Continuous-spontaneous-reduction model involving gravity*, Physical Review A **42**, 1057 (1990).
- [9] M. Zych, F. Costa, I. Pikovski, and v. Brukner, *Quantum interferometric visibility as a witness of general relativistic proper time*, Nature Communications **2**, 505 (2011).
- [10] R. Colella, A. W. Overhauser, and S. Werner, *Observation of gravitationally induced quantum interference*, Phys. Rev. Lett. **34**, 1472 (1975).
- [11] B. E. A. Saleh and M. C. Teich, *Fundamentals of Photonics*, Wiley (1991).
- [12] J. D. Franson, *Bell inequality for position and time*, Phys. Rev. Lett. **62**, 2205 (1989).
- [13] W. Tittel, J. Brendel, H. Zbinden, and N. Gisin, *Violation of Bell Inequalities by Photons More Than 10 km Apart*, Physical Review Letters **81**, 3563 (1998).
- [14] G. Lima, G. Vallone, A. Chiuri, A. Cabello, and P. Mataloni, *Experimental Bell-inequality violation without the postselection loophole*, Phys. Rev. A **81**, 2 (2010).
- [15] G. Carvacho, J. Cariñe, G. Saavedra, A. Cuevas, J. Fuenzalida, F. Toledo, M. Figueroa, A. Cabello, J.-A. k. Larsson, P. Mataloni, G. Lima, and G. B. Xavier, *Postselection-Loophole-Free Bell Test Over an Installed Optical Fiber Network*, Physical Review Letters **115**, 030503 (2015).
- [16] J. Brendel, N. Gisin, W. Tittel, and H. Zbinden, *Pulsed Energy-Time Entangled Twin-Photon Source for Quantum Communication*, Phys. Rev. Lett. **82**, 2594 (1999).
- [17] N. Gisin, G. Ribordy, W. Tittel, and H. Zbinden, *Quantum cryptography*, Reviews of Modern Physics **74**, 145 (2002).
- [18] P. Villoresi, T. Jennewein, F. Tamburini, M. Aspelmeyer, C. Bonato, R. Ursin, C. Pernechele, V. Luceri, G. Bianco, A. Zeilinger, and C. Barbieri, *Experimental verification of the feasibility of a quantum channel between space and Earth*, New Journal of Physics **10**, 033038 (2008).
- [19] G. Vallone, D. Bacco, D. Dequal, S. Gaiarin, V. Luceri, G. Bianco, and P. Villoresi, *Experimental Satellite Quantum Communications*, Physical Review Letters **115**, 040502 (2015).